Applied Research Frontiers

Ariviyal Publishing

Research Article

DOI: 10.36686/Ariviyal.ARF.2022.01.03.015

Appl. Res. Front., 2022, 1(3), 17-21.

Sintering of α-Alumina in Powder Form and Characterization of Some Mechanical Properties

Erdem UZUN,*[a] and Yasemin YILDIZ YARAR[b]

[a]*Department of Physics, Kamil Özdağ Faculty of Science, Karamanoğlu Mehmetbey University, 70100-Karaman, Turkey.*
[b]*Department of Physics, Faculty of Arts & Science, Yıldız Technical University, 34220-stanbul, Turkey.*

***Corresponding author E-mail address**: erdemuzun@kmu.edu.tr (Erdem UZUN)*; yarar@yildiz.edu.tr (Yasemin YILDIZ YARAR)

ISSN: 2583-3065

Crossref

Publication details
Received: 26th October 2022
Revised: 21st December 2022
Accepted: 21st December 2022
Published: 30th December 2022

Abstract: Some sintering properties of α-alumina in powder form were investigated and the effects of sintering temperature on some mechanical properties were tested. Alumina powders were moistened with distilled water, granulated, pressed and sintered. The best granulation rate has been achieved with a moisture content of 6%. Pressed α-alumina powders were fully sintered at temperatures of 1550°C and above. In sintered samples, water absorption and surface porosity were not observed, and moreover 98% of the theoretical density was achieved. Hardness, fracture toughness and fracture strength of the sintered samples were measured. Moreover, the colour of alumina ceramics changes from white to cream with increasing sintering temperature.

Keywords: alumina; sintering; harness; fracture toughness

1. Introduction

Ceramic materials have become the main inputs of industrial fields such as construction, machinery, electric, electronics, energy, and communication technologies due to their superior properties such as resistance to heat and wear (chemical-mechanical), electrical shocks, and radiation damage.[1,2] On the other hand, fragility is the most important disadvantage that restricts the use of ceramics. Metal oxides, silicates, carbides, nitrides, borides, beryllides, aluminides, titanites, zirconides, sulfurides, and tellurides, as well as glass and cement type materials, can be considered as ceramics. However, composite ceramics can be produced by using ceramic compounds among themselves or together with other metal or polymer materials.

Alumina, which is among the high-tech materials, is still attractive and being studied extensively. In this study, α-alumina (α-Al_2O_3), which is widely used in the production of glass, biomaterials, laboratory equipment, high temperature furnaces, cutting tools, bedding materials, textile industry and electronic circuit pads was investigated.[3,4]

The most important process that determines the final properties in ceramic material production is sintering.[2–4] Alumina powders come into contact with each other by being compressed with the help of mechanical pressure during shaping. Besides, the sintering process is applied to eliminate porosity in the material and to obtain a compact structure.[3,4]

Sintering can be applied by heating the material at once or in steps, as well as under pressure or under different atmospheric conditions.

Lin et al.,[5] and many other researchers[6–8] sintered alumina powders both at once and/or in two steps, reporting that two-step sintering reduces particle size and increases bulk density. Average particle size and distribution,[9,10] particle shape and surface charges,[10] sintering time,[11] as well as increasing the pressing pressure in the forming phase[12] affects density. Lv et al.[13] and Lóh et al.[8] have suggested that the reduction in particle size and homogeneous distribution lead to an improved hardness and fracture toughness. Similar results have been reported by other researchers as well.[6,8,9,11,14–17]

Dimensions of a sintered material decreases approximately 15-20%, which in return decreases the porosity and increases the material density.[11,18] Moreover, previously sintered and ground CT3000SG quality alumina was re-sintered by Lv et al.[13] and as a result, reported that a linear shrinkage reduction of 7.8% was observed in material dimensions. Moreover, the colour of the sintered alumina changes with respects to the sintering temperature. Previously published studies show that the parameters that determine the colour of alumina are related to its crystal structure and change with the crystallization proportion in the material.[19,20]

Table 1. Chemical composition of the alumina

Impurities	%
Na_2O	0.08
Fe_2O_3	0.02
SiO_2	0.03
CaO	0.02
MgO	0.07

Table 2. Specific surface area, and powder size analyses of the alumina

Properties / method	Unit	Value
Specific Surface Area / BET	m^2/g	7.5
Particle Size / D50 cilas	µm	2.5
Particle Size / D90 cilas	µm	2.0

Krell et al.[21] claimed that as the particle size decreased, the light transmittance of alumina increased. Ghanizadeh et al.[15] reported that the light transmittance of alumina with an average particle size of ~ 0.32 µm is ~ 80%. Besides, Apetz and Bruggen[22] and Stuer et al.[23] suggested that particle size distribution and porosity also affect the change in the colour of the ceramics. On the other hand, if the sintering temperature is close to the material's melting point, the form of the ceramic material may deteriorate. Previously published studies show that alumina is sintering generally up to 1650°C.[24] In this study, samples in different geometries were produced using calcined alumina in powder form, and some mechanical properties after the sintering at different temperatures were investigated.

2. Material and Method

2.1. Raw Material

In this study, ALCOA CT 3000 SG quality calcined alumina powders were used. Chemical composition, specific surface area, and powder size analyses of the alumina were given in Table 1 and 2.

2.2. Moistened, Granulation and Pressing

The powder material was moistened with distilled water and formed into granules smaller than 425 µm. The optimum moisture content of alumina is determined as 6 wt.% for granulation. Disc (with 23.25 mm diameter) and rectangular (with 40 mm × 8 mm dimensions) shaped heat-treated steel moulds were used for the forming process. Before each pressing, the surfaces of the mould were cleaned with a stearic acid-acetone solution to ensure easy removal of the samples from the mould. 4 g of alumina in the disc-shaped mould and 5 g of alumina in the rectangular-shaped mould were pressed within 1s by applying a load of 103 kg/cm^2.

2.3. Drying and Sintering Process

The pressed samples were allowed to dry at room temperature (20±1°C) for 24 hours. The green density of the dried samples was calculated by using the mass-volume relationship. Green density provides information on how much the ceramic material that has not yet been sintered will shrink when fully sintered.[25] Then, all the samples were separated into numerous groups and heated up to previously determined sintering temperatures with a constant heating rate of 3°C/min and in air atmosphere. The 1st group was sintered at 1200°C for 1 hour, 2nd group was sintered at 1550°C for 1 hour, 3rd group was sintered at 1600°C for 1 hour, and the 4th group was sintered at 1650°C for 1 hour. Following the sintering, all samples were cooled down to the room temperature. It was observed that samples treated at 1200°C were only partly sintered whereas all other samples were sintered completely.

2.4. Sintered Sample Tests

The bulk density of the sintered samples was measured by the Archimedes principle. Hardness measurements were performed by ASTM C1327-15[26] standard using Vickers micro hardness device. Fracture toughness (K_{IC}) was measured by the Trace Crack Length method[27] and fracture strength was measured by the Three-Point Bending Test in ASTM C1161-18[28] standards. A wet grinding sequence was applied to ceramic surfaces by SiC emery paper with grit sizes of 400 and 800, respectively. Subsequently, the samples were polished with diamond paste of 6µ, chemical etched by boiling in concentrated HF for 2 hours, and finally heat etched at 1400°C for 1 hour.

3. Results and Discussions

3.1. Green Density of the Un-Sintered Samples

The green density of the un-sintered disc and rectangular-shaped samples was calculated by using the relationship between mass - volume. The radii and thicknesses of the 10 pressed and dried disc shaped samples as well as the dimensions (length, width and thickness) of the 20 rectangular-shaped samples were measured. The green density of the disc and rectangular-shaped samples were calculated as 2.35 ± 0.02 $g.cm^{-3}$ and 2.54 ± 0.02 $g.cm^{-3}$, respectively.

3.2. Sintering Shrinkage

The radii of the 10 disc-shaped samples were measured before (r_{raw}) and after (r_{sin}) sintering at 1600°C. Besides, the dimensions of the 20 rectangular-shaped samples were measured before and after sintering at 1600°C. The linear sintering shrinkage (%) and total volume shrinkage were calculated with the equations given below:

$$Linear\ Sintering\ shrinkage\ (\%) = 100 \times (L_{raw} - L_{sin})/L_{raw} \quad (1)$$

$$Total\ Volume\ Shrinkage\ (\%) = 100 \times (V_{raw} - V_{sin})/V_{raw} \quad (2)$$

Each dimension was measured 5 times and the average values of the measurements were used for the calculations. Where L_{raw} is the sample length after drying, while L_{sin} is the final length after sintering; V_{raw} is the volume calculated after drying, while V_{sin} is the volume calculated after sintering. Results show that sintered disc-shaped samples shrunk approximately 23% in diameter, 19% in thickness, and 41% in volume. Similarly, the average shrinkage in length, thickness, width, and volume of the sintered rectangular-shaped samples were calculated as 16%, 15%, 12%, and 37%, respectively.

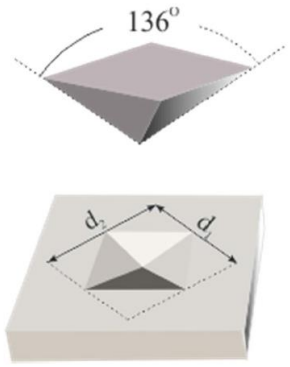

Fig. 1. Vickers micro hardness experimental setup.

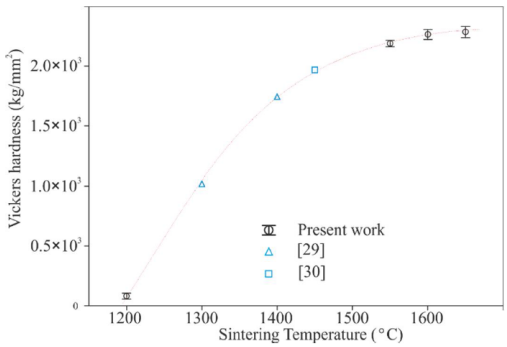

Fig. 2. The effect of sintering temperature on HV hardness.

3.3. Colour Change by Sintering

In order to determine the colour change with respect to the sintering temperature, the colours of the un-sintered and sintered samples were examined by the bare eye. A strong correlation between the colorization and the calcination temperature is noted. It is observed that the colour of un-sintered alumina was white; whereas the colour of partly sintered at 1200°C was white; while that of 1550°C, 1600°C and 1650°C became darker.

3.4. Bulk Density, Open Porosity and Water Absorption

Firstly, sintered disc and rectangular-shaped samples were boiled and kept in distilled water for 4 hours and at least 4 days, respectively. The masses of the samples in water were weighed as M_{wat} and then their surfaces were cleaned by a wet cotton cloth and weighed again (M_{wet}). Lastly, the samples were dried in the oven for 2 hours at 110°C and weighed as M_{dry}. Bulk density, open porosity and water absorption values were calculated by using the following equations;

$$Bulk\ Density\ (g.cm^{-3}) = 100 \times M_{dry}/(M_{wet} - M_{wat}) \quad (3)$$

$$\text{Open Porosity (vol. \%)} = 100 \times (M_{wet} - M_{dry})/(M_{wet} - M_{wat}) \quad (4)$$

$$\text{Water Absorption (wt. \%)} = 100 \times (M_{wet} - M_{dry})/M_{dry} \quad (5)$$

The results showed that there was no water absorption and no open porosity (0%) in the disc and rectangular-shaped samples. However, the bulk density for both types of samples was calculated as 3.91 ± 0.03 g.cm^{-3} by Archimedes principle.

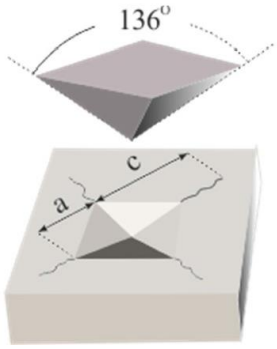

Fig. 3. Vickers fracture toughness experimental setup.

Fig. 4. SEM images of traces and cracks created on the sample surface.

3.5. Surface Roughness

The surface roughness of the samples was measured by using Mitutoyo SJ-210 electronic surface roughness measuring device. For the process, disc-shaped specimens, onto which no surface treatment was applied, were selected. The surface roughness of the materials was measured as 0.5 µm by moving the sensitive tip of the device over the material. This is a very satisfactory result for unpolished ceramic surface roughness.

3.6. Hardness Measurements (HV)

The hardness of ceramic materials was measured using a Vickers micro hardness device. In this test, square based pyramidal diamond indenter with a sharp tip and an apex angle of 136° is pressed on the specimen's surface (Fig. 1). The pyramidal diamond indenter forms a rhombus on the surface of the ceramic. The two diagonals of the permanent rhombus were measured using a light microscope and Vickers micro hardness number (HV) was calculated with the help of Equation 6 according to ASTM C1327-15[26] standard. Here, d1 and d2 are the lengths of two diagonals of the permanent rhombus. In HV experiments, permanent rhombus was created by applying 1 kg of load on the sample surface for 20s. HV values were calculated by taking 5 traces from each sample separately, and results were given with some literature.[29,30] The change of the hardness of the samples with the sintering temperature can be seen in Fig. 2.

$$HV = 2.P.Sin(68)/([d1 + d2]/2)^2 \quad (6)$$

3.7. Fracture Toughness

Fracture toughness of disc-shaped samples was measured by the Trace Crack Length method 27 (See Fig. 3). Samples sintered at 1600°C were polished and 20s 5 kg trace load was applied to the surface by Vickers micro hardness device. 4 different permanent

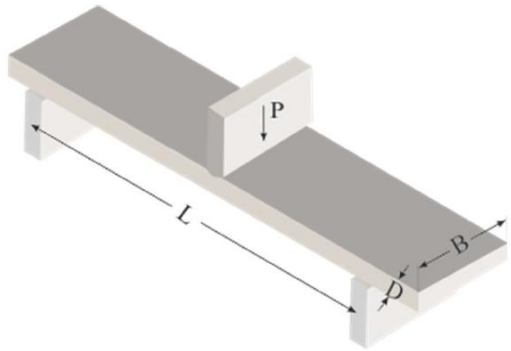

Fig. 5. Three-point fixture configuration.

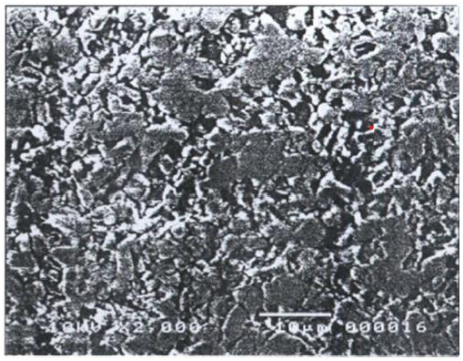

Fig. 6. SEM image of an alumina sintered at 1600°C.

rhombuses were formed on each sample surface and their trace crack dimensions were measured. SEM images of the trace-cracks were captured, their dimensions were measured and fracture toughness was calculated as (0.46 ± 0.01) × 10^6 Kg $\sqrt{m}/m^2$ by using Equation 7. Here, P is applied trace load, a is the length of diagonal of the rhombus and c is the sum of cracks length and the a. SEM images used for the measurement of the trace-cracks dimensions are given in Fig. 4.

$$K_{IC} = 0.079\ (P/a^{3/2}) \log\ (4.5\ a/c) \quad (7)$$

3.8. Flexural Strength

Flexural strength was measured by the Three Point Bending test according to ASTM C1161-18[28] standard. In the bending test, a load was applied to the rectangular-shaped samples shown in Fig. 5 until they break at their mid-points. The flexural strength was calculated with the help of Equation 8 by measuring the critical load breaking the sample and the sample dimensions. Here, P is applied load, L is outer (support) span, B is sample width, and d is sample thickness. The measurements were repeated for 4 samples, and the average breaking strength and standard error were calculated as (26 ± 8) × 10^6 kg/m^2.

$$S = 3\ P\ L\ /(2\ B\ D^2) \quad (8)$$

3.9. Surface Morphology

According to the SEM investigations (see Fig. 6), the microstructure of the alumina sintered at 1600°C depict no homogeneity. The appearing contrasts in the SEM image originate from the difference of reflectivity along the ceramic surface. This can be due to the influence of the surface roughness and the presence of open pores. It was seen that there were compact regions where grain sizes are larger than 10 μm. However, grain boundaries and sizes are not uniformly distributed along the entirety of the volume and there are micro-voids and pores between grains. Inhomogeneous microstructures can appear when ceramic materials are sintered at one step.[5,8,13,24]

4. Conclusions

In this study, various sintering properties of α-alumina ceramics and the effects of sintering temperature on certain mechanical properties were investigated. In order to achieve the best pressing rate of the granules, it is important to determine the optimum value of the moisture. The best granulation rate was achieved with a moistening of 6 wt.%. Fundamental pressing problems such as material adhesion on the mould surface, pressed pellet breakage and dispersion are minimized by cleaning the mould surfaces using stearic acid-acetone solution. It has been observed that ALCOA CT 3000 SG quality alumina is completely sintered at a temperature of 1550°C and above. Linear sintering shrinkage of the alumina sintered at 1600°C was measured as 14-16% and total volume shrinkage were measured as 37-41%. The bulk density of the sintered alumina was calculated as 3.91 ± 0.03 g/cm^3. This equals to the 98% of the theoretical density of alumina (3.98 g/cm^3). Open porosity and water absorption were not measured for alumina sintered at 1600°C. Furthermore, it was observed that the colour of alumina changed from white to cream with respect to the increasing sintering temperature. The darkening of the colour of the samples is strongly dependent on the calcination temperature. The darkening can be related to an increased amount of crystallization.

It was also observed that the Vickers hardness of the investigated samples increased with respect to the increasing sintering temperature.

Fracture toughness and breaking strength of the materials were measured as (0.46 ± 0.01) × 10^6 kg $\sqrt{m}/m^2$ and (26 ± 8) × 106 kg/m^2, respectively. The measured results are in agreement with the literature values.

Conflicts of Interest

The authors declare no conflict of interest.

References

1 Doğan Ş. Açıklamalı Seramik Teknolojileri. *Birsen Yayınevi, İstanbul,* 1985.
2 Geçkinli A.E. *İleri teknoloji malzemeleri*. İstanbul Teknik Üniversitesi, 1991.
3 Hart L.D. Alumina Chemicals. Wiley: Westerville, Ohio, 1990.
4 Chiang Y.-M.; Birnie D.P.; Kingery W.D. Physical Ceramics; Wiley: New York, NY, 1997.
5 Lin F.J.; De Jonghe L.C.; Rahaman M.N. Microstructure Refinement of Sintered Alumina by a Two-step Sintering Technique. *J. Am. Ceram. Soc.*, 1997, **80**, 2269-2277. [CrossRef]
6 Wachtman J.B.; Cannon W.R.; Matthewson M.J. *Mechanical Properties of Ceramics*. John Wiley & Sons, 2009. [Link]

7 Lóh N.J.; Simão L.; Jiusti J.; De Noni Jr A.; Montedo O.R.K. Effect of Temperature and Holding Time on the Densification of Alumina Obtained by Two-step Sintering. *Ceram. Int.*, 2017, **43**, 8269-8275. [CrossRef]
8 Lóh N.J.; Simão L.; Jiusti J.; Arcaro S.; Raupp-Pereira F.; De Noni Jr A.; Montedo O.R.K. Densified Alumina Obtained by Two-step Sintering: Impact of the Microstructure on Mechanical Properties. *Ceram. Int.*, 2020, **46**, 12740-12743. [CrossRef]
9 Krell A.; Blank P. Grain Size Dependence of Hardness in Dense Submicrometer Alumina. *J. Am. Ceram. Soc.*, 1995, **78**, 1118-1120. [CrossRef]
10 Krell A.; Blank P. The influence of Shaping Method on the Grain Size Dependence of Strength in Dense Submicrometre Alumina. *J. Eur. Ceram. Soc.*, 1996, **16**, 1189-1200. [CrossRef]
11 Shen Z.; Johnsson M.; Zhao Z.; Nygren M. Spark Plasma Sintering of Alumina. *J. Am. Ceram. Soc.*, 2002, **85**, 1921-1927. [CrossRef]
12 Eskandari A.; Aminzare M.; Aboutalebi S.H.; Sadrnezhaad S.K. Effect of High energy Ball Milling on Compressibility and Sintering Behavior of Alumina Nanoparticles. *Ceram. Int.*, 2012, **38**, 2627-2632. [CrossRef]
13 Lv L.; Lu Y.; Zhang X.; Chen Y.; Huo W.; Liu W.; Yang J. Preparation of Low-shrinkage and High-Performance Alumina Ceramics via Incorporation of Pre-sintered Alumina Powder based on Isobam Gelcasting. *Ceram. Int.*, 2019, **45**, 11654-11659. [CrossRef]
14 Skrovanek S.D.; SD S.; RC B. Microhardness of a Fine-grain-size Al_2O_3. 1979. [CrossRef]
15 Ghanizadeh S.; Grasso S.; Ramanujam P.; Vaidhyanathan B.; Binner J.; Brown P.; Goldwasser J. Improved Transparency and Hardness in α-Alumina Ceramics Fabricated by High-pressure SPS of Nanopowders. *Ceram. Int.*, 2017, **43**, 275-281. [CrossRef]
16 Nečina V.; Pabst W. Influence of the Heating Rate on Grain Size of Alumina Ceramics Prepared via Spark Plasma Sintering (SPS). *J. Eur. Ceram. Soc.*, 2020, **40**, 3656-3662. [CrossRef]
17 Rice R. Particle and Grain Effects on Mechanical Properties of Composites at Elevated Temperature. In Mechanical Properties of Ceramics and Composites; CRC Press: 2000, 619–656, New York, USA. [Link]
18 Greil P. Near Net Shape Manufacturing of Ceramics. *Mater. Chem. Phys.*, 1999, **61**, 64-68. [CrossRef]
19 Wang S.; Wei X.; Gao H.; Wei Y. Effect of Amorphous Alumina and α-Alumina on Optical, Color, Fluorescence Properties and Photocatalytic Activity of the $MnAl_2O_4$ Spinel Oxides. *Optik*, 2019, **185**, 301-310. [CrossRef]
20 Gao H.; Yang H.; Wang S.; Li D.; Wang F.; Fang L.; Lei L.; Xiao Y.; Yang G. A New Route for the Preparation of $CoAl_2O_4$ Nanoblue Pigments with High Uniformity and its Optical Properties. *J. Sol-Gel Sci. Technol.*, 2018, **86**, 206-216. [CrossRef]
21 Krell A.; Blank P.; Ma H.; Hutzler T.; Nebelung M. Processing of High-density Submicrometer Al_2O_3 for New Applications. *J. Am. Ceram. Soc.*, 2003, **86**, 546-53. [CrossRef]
22 Apetz R.; Van Bruggen M.P. Transparent Alumina: A Light-scattering Model. *J. Am. Ceram. Soc.*, 2003, **86**, 480-486. [CrossRef]
23 Stuer M.; Bowen P.; Cantoni M.; Pecharroman C.; Zhao Z. Nanopore Characterization and Optical Modeling of Transparent Polycrystalline Alumina. *Adv. Funct. Mater.*, 2012, **22**, 2303-2309. [CrossRef]
24 Uzun, E. Characterization of Thermoluminescent Properties of Seydisehir Alumina and Investigation of Properties of Dose Response, Ms Thesis, Yildiz Technical University: Istanbul, 2008. [Link]
25 DeHoff R.T.; Kuczynski G.C.; Miller A.E.; Sargent G.A. Sintering and Heterogeneous Catalysis. 1984. [CrossRef]
26 Standard Test Method for Vickers Indentation Hardness of Advanced Ceramics. ASTM C1327-15; West Conshohocken, PA, 2019. [Link]
27 Ponton C.B.; Rawlings R.D. Vickers Indentation Fracture Toughness Test Part 1 Review of Literature and Formulation of Standardised Indentation Toughness Equations. *Mater. Sci. Technol.*, 1989, **5**, 865-872. [CrossRef]
28 Standard Test Method for Flexural Strength of Advanced Ceramics at Ambient Temperature. A. ASTM C1161-18, 2018. [Link]
29 Pulgarin H.L.C.; Albano M.P. Sintering, Microstrusture and Hardness of Different Alumina–Zirconia Composites. *Ceram. Int.*, 2014, **40**, 5289-5298. [CrossRef]
30 Wang C.J.; Huang C.Y. Effect of TiO_2 Addition on the Sintering Behavior, Hardness and Fracture Toughness of an Ultrafine Alumina. *Mater. Sci. Eng.: A*, 2008, **492**, 306-310. [CrossRef]